Analysis of trends and sudden changes in long-term environmental data from King George Island (Antarctica): relationships between global climatic oscillations and local system response

A. Valeria Bers · Fernando Momo · Irene R. Schloss · Doris Abele

Abstract The Western Antarctic Peninsula is one of the most rapidly warming regions on earth. It is therefore important to analyze long-term trends and inter-annual patterns of change in major environmental parameters to understand the process underlying climate change in Western Antarctica. Since many polar long-term data series are fragmented and cannot be analysed with common time series analysis tools, we present statistical approaches that can deal with missing values. We applied *U-statistics* after Pettit and Buishand to detect abrupt changes, dynamic factor analysis to detect functional relationships, and additive modelling to detect patterns in time related to climatic cycles such as the Southern Annular Mode and El Niño Southern Oscillation in a long-term environmental data set from King George Island (WAP), covering 20 years. Our results not only reveal sudden changes for sea surface temperature and salinity, but also clear patterns in all investigated variables (sea surface temperature, salinity, suspended particulate matter and Chlorophyll *a*) that can directly be related to climatic cycles. Our results complement previous findings on climate related changes in the King George Island Region and provide insight into the environmental conditions and climatic drivers of system change in the study area. Hence, our statistical

A. V. Bers (✉) · D. Abele
Alfred Wegener Institute for Polar and Marine Research, Am Handelshafen 12, 27570 Bremerhaven, Germany
e-mail: Valeria.Bers@awi.de

F. Momo
Institute of Sciences, National University of General Sarmiento, Juan M. Gutiérrez 1150, Los Polvorines, Buenos Aires, Argentina

I. R. Schloss
Instituto Antártico Argentino, Cerrito 1248 (C1010AAZ), Ciudad Autónoma de Buenos Aires, Argentina

I. R. Schloss
CONICET, Buenos Aires, Argentina

I. R. Schloss
Institut des sciences de la mer de Rimouski, 310, Allée des Ursulines, G5L 3A1, Rimouski, Québec, Canada

© Springer

analyses may prove valuable for other polar environmental data sets and contribute to a better understanding of the regional variability of climate change and its impact on coastal systems.

1 Introduction

With a surface air temperature warming rate of 3.7±1.6 °C per century, the Western Antarctic Peninsula (WAP) belongs to the most rapidly warming regions on earth (Vaughan et al. 2003; Turner et al. 2005). Especially the maritime western region of the peninsula with its small (compared to temperate regions) but distinct seasonal climate oscillations and summer temperatures close to the melting points of large ice masses (Vaughan 2006) has become a showcase area to study the response to climate change of Antarctic ice masses and coastal biota (Smith et al. 2008; Clarke et al. 2009). Major changes in coastal and shelf systems are becoming evident in the timing and duration of the annual sea ice cover (Ducklow et al. 2007; Schofield et al. 2010; Stammerjohn et al. 2008), but also in a rise of surface water temperatures (Meredith and King 2005). The inter-annual climate variability along the WAP is remarkable (Orr et al. 2008) and mainly driven by the Southern Annual Mode (SAM) and the El Niño Southern Oscillation (ENSO) (Schloss et al. 2012; Fogt et al. 2011; Meredith et al. 2008; Stammerjohn et al. 2008).

The SAM index describes the atmospheric variability between the mid- and high-latitude surface pressure (Gong and Wang 1999) and explains ~35 % of the total southern hemisphere climate variability (Marshall 2007). Since the WAP stretches out into much lower latitudes than the rest of the Antarctic continent, the SAM is particularly important for the climatic variability in this area (Marshall 2007; Russell and McGregor 2010). The recent warming trend at the WAP can be attributed to a shift towards a positive phase of the SAM since the mid-1960s, resulting in an observable strengthening of the circumpolar westerly winds (Marshall 2002; Orr et al. 2008; Gillet et al. 2006; Monaghan et al. 2008) which drives warmer circumpolar deep water onto the western peninsula shelf. Furthermore, the WAP region is strongly influenced by the tropical El Niño Southern Oscillation (ENSO) (Fogt et al. 2011; Russell and McGregor 2010): while El Niño conditions lead to colder periods along the WAP, La Niña conditions cause warming, including both a delay of sea ice formation and sea ice duration (Stammerjohn et al. 2008). This is especially true when ENSO is in-phase with SAM (Fogt et al. 2011; Russell and McGregor 2010).

King George Island (KGI), the largest of the South Shetland Islands (−62.0333, −58.3500), is located at the northern tip of the WAP (Fig. 1). The Argentine research station Carlini (former Jubany Station), with the German-Argentine collaborative Dallmann laboratory (run by AWI, IAA and co-financed by the Dutch NWO), offers a unique platform in terms of both systematic and interdisciplinary research to investigate the drivers and ecological consequences of global change in coastal Antarctica. The platform in Potter Cove has by now been continuously active for more than 20 years. At King George Island, the rapidly increasing air temperatures have resulted in a dramatic retreat of the local glacier fronts and loss of ice mass, especially in the lower tidewater parts of the glaciers <270 m above sea level (Blindow et al. 2010; Rückamp et al. 2011). Glacier melt water run-off carries high particle loads into the coastal areas around the island (Eraso and Dominguez 2007), and, consequently, sedimentation of eroded material from tributary inlets such as Potter and Marian Cove into Maxwell Bay have almost tripled since the 1940s (Monien et al. 2011), with implications for benthic and pelagic systems (Schloss et al. 1999; Pakhomov et al. 2003; Tatian et al. 2008). In November 1991 systematic recordings of hydrological and biological parameters started in Potter Cove and have continued to the present. Measurements of sea surface temperature, salinity, Chlorophyll a and total suspended particulate matter concentrations are conducted from rubber boats, following a weekly to bi-weekly (summer) and monthly (winter) sampling pattern. Weather conditions at Carlini station (i.e. sea ice formation preventing the
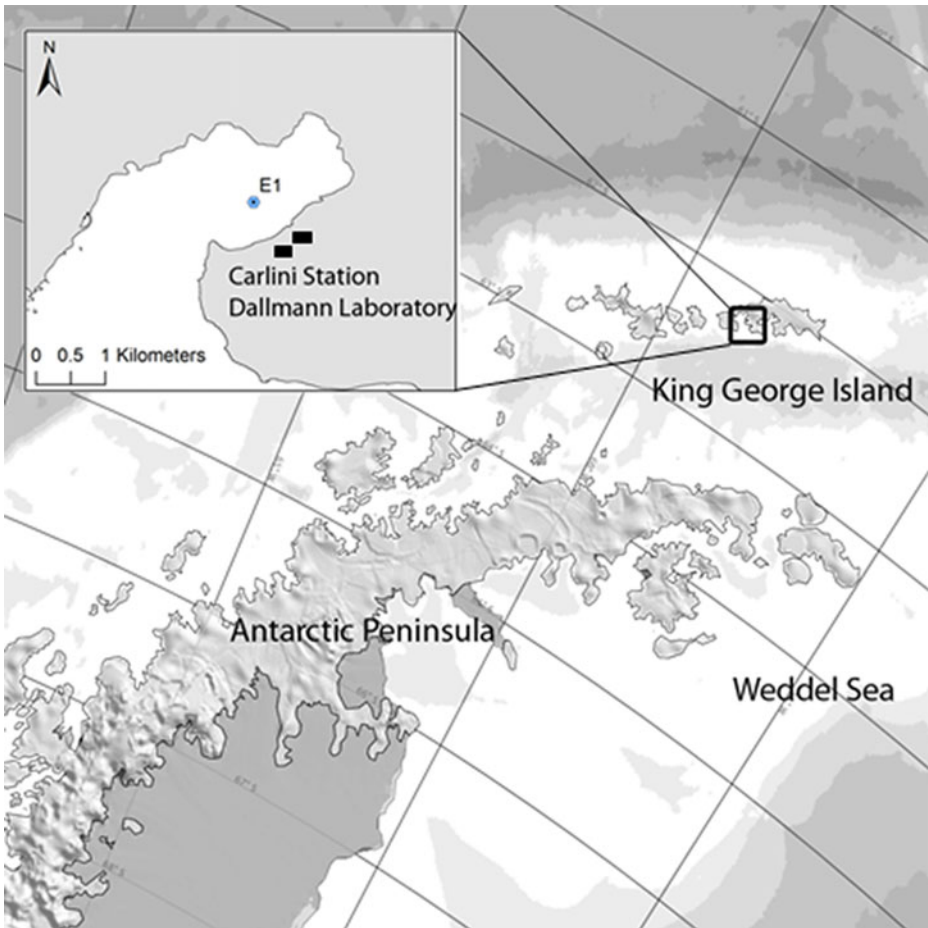
Fig. 1 Geographical location of Potter Cove, King George Island, and location of the study site E1. Map source: SCAR Antarctic Digital Database

sampling procedure) and logistical constraints to the regular sampling procedure have caused short but also longer gaps, with missing values in the data series, especially in the austral winter months, whereas air temperature has been continuously measured since 1991 until the present (Fig. 2). Most common types of times series analyses, such as spectral analysis or ARIMA are not applicable, since they require complete data sets, and often even longer time-scales. Recently, Schloss et al. (2012) analysed the same dataset (November 1991–December 2009) and presented a first general trend analysis and cross-correlations to determine long-term climatic trends. In contrast, the objective of the present paper is to reveal sudden changes in the investigated parameters related to the major climatic cycles, for a better understanding of climate related dynamics caused by SAM and ENSO in a small scale coastal Antarctic system. The analysis aims at explaining some of the previously described non-linear trends and patterns in the data set (Schloss et al. 2012). To this end, we chose to apply specific tests of turning points and analyses of non-linear trends, combining all measured parameters with the climatic indices to an advanced version of this unique data set (now extended until December 2010).
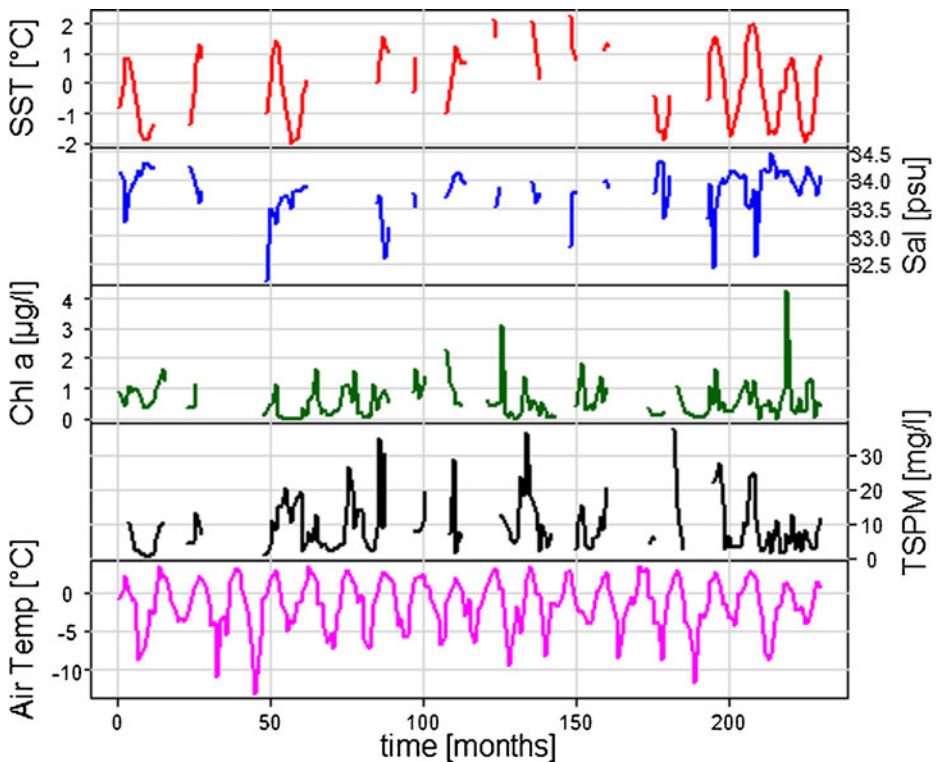
Fig. 2 Monthly means of environmental data available in this study: sea surface temperature (SST), salinity, total suspended particulate matter (TSPM), Chlorophyll *a* (Chl *a*) and air temperature. Air temperature values are de-seasonalized after LOESS

2 Material & methods

Sea surface temperature (SST), salinity, total suspended particulate matter (TSPM) and Chlorophyll *a* concentration (Chl *a*) data from November 1991 to December 2010 (230 month in total) were used in this study (doi:10.1594/PANGAEA.745597, doi:10.1594/PANGAEA.745596, doi:10.1594/PANGAEA.745598). Samples were taken at station E1 (−62.2321; −58.6665) in Potter Cove close to Carlini station (Fig. 1). Monthly means of the values of each variable in surface waters (0–10 m) were calculated and used in the statistical analyses. Air temperature data were obtained from the Servicio Meteorológico Nacional, Argentina. We used the Southern Annular Mode (SAM) index and the bivariate ENSO time series (BEST) index (Smith and Sardeshmukh 2000), to evaluate the influence of climatic cycles on the KGI system. The BEST ENSO index was chosen since it combines the oceanic component of the ENSO phenomenon (ENSO 3.4 index) with an atmospheric component, i.e. the Southern Oscillation index. The SAM index was obtained from the Joint Institute for the Study of the Atmosphere and Ocean (JISAO), University of Washington, the BEST ENSO index from the Earth System Research Laboratory (ESRL) of the National Oceanographic and Atmospheric Administration (NOAA). Our TSPM data set was complemented with TSPM measurements of Station L1 (−62.2358, −58.6634 of Philipp (2010)), approx. 440 m apart from our sampling station. Two types of analyses of change were performed with the data: i) detection of sudden changes, and ii) trends over time.

2.1 U-statistics: detecting abrupt changes

Time series may have no clear trends, but they can contain sudden changes of average in some points, i.e. the average value of the variable can be different before and after a certain point without a slight trend of change. Because climate and ecological systems are not linear, it is possible that local or regional variables respond in an abrupt way to general oscillations or tendencies. To explore and eventually detect these kind of changes in each measured variable we used two statistical methods: the Buishand U-statistics (Buishand 1984) and the Pettitt U_t (Pettitt 1980, 1981).

The cumulative deviation test (Buishand 1984) is based on the rescaled cumulative sum (CUSUM) of the deviation from the mean. The test is relatively sensitive to change-points that occur towards the center of the time series (Kundzewicz and Robson 2004), but has shortcomings if the series contains obvious outliers because that can produce high (and apparently significant) values which do, however, not correspond to real average change (Kiely et al. 1998). The series analyzed here have no evident outliers and the method can be applied without problems. The statistic U after Buishand (1984) was calculated as:

$$U = [n(n+1)]^{-1} \sum_{k=1}^{n-1} \left(S_k^* / D_y \right)^2$$

with $S_k^* = \sum_{i=1}^{k} (yi - \bar{y})$ and D_y the sample standard deviation.

The null hypothesis of this test is the absence of a sudden change in the time series. In the case of rejection of the null hypothesis, no approximation of the date of the change is proposed by this test. Critical values and bounds for the statistic U are listed in Buishand (1984). Further, in order to test the statistical significance and to determine the turning point in the time series, a particular form of the non-parametric Mann–Whitney test, developed by Pettitt (1980), was applied. In this rank-based test the null hypothesis is the absence of a turning point in the sequence (x_i):

$$U_t = \sum_{i=1}^{t} \quad \sum_{j=t+1}^{T} \text{sign}(x_i - x_j),$$

where sign $(x) = -1$ if $(x_i - x_j) < 0$; 0 if $(x_i - x_j) = 0$; and $+1$ if $(x_i - x_j) > 0$.

A time series with no turning point would result in a continuously increasing value of U_t. In case of existing turning points, the Pettitt U_t shows local maximum values in the time series for these points. This test is extremely useful for detecting shifts in the median of a sample series with unknown turning point, since, in any case, it provides the most probable changing point of the series, which corresponds to the greatest U_t value in the sequence (Caloiero et al. 2011). U_t values were calculated for each available monthly mean of the different variables and subsequently plotted to visualize the turning points (Fig. 2a–d). In a series of N data, with t varying between 1 and $N-1$, the probability of U_t higher than a given value k is

$$P(U_t > k) \approx 2 \exp\left[-6k^2 / \left(N^3 - N^2\right)\right]$$

While rank-based tests have the advantage that they are robust and easy to use, they are usually less powerful than a parametric approach (Kundzewicz and Robson 2004). All calculations of U-statistics were performed in Microsoft Excel using the available monthly means of each variable (SST, Salinity, TSPM and Chl a, cf. Table 2). Monthly means of SST were deseasonalized using the standard procedure according to Cleveland et al. (1990) in Brodgar (v.2.6.6, www.brodgar.com) to eliminate the strong seasonal signals.

2.2 Additive modeling

To explore the existence of potential functional relationships between measured variables (SST, salinity, TSPM, Chl *a*) and potential explanatory ones (air temperature, SAM and/or ENSO) we used generalized additive modeling (GAM). GAMs were introduced by Hastie and Tibshirani (1986) and describe general linear models with a linear predictor involving a sum of smoothing functions of covariates (Wood 2006). The additive model fits a smoothing curve through the data to link response and explanatory variables. Estimation of smoothers is done using a method called a back-fitting algorithm (Zuur et al. 2009). We applied GAMs with a Gaussian distribution and identity-link function for each of the measured response variables with "year" as a smoothing function *s(year)*. The analysis was performed with the Brodgar software (v.2.6.6), based on the mgcv package in R (Wood 2006). The mgcv package generally uses smoothing splines and does cross-validation to determine the optimal amount (i.e. the effective degrees of freedom) of smoothing (Wood 2006; Zuur et al. 2009).

2.3 Dynamic factor analysis (DFA)

To confirm whether the present environmental time series bears any general patterns over time, and whether the measured variables are related to climatic cycles such as SAM or ENSO, a dynamic factor analysis (DFA) after (Zuur et al. 2003) was performed using the software Brodgar (v. 2.6.6). DFA is a method to estimate "trends" that are common to all series, as well as the effects of explanatory variables and interactions in a multivariate time series data set that may even contain missing values (Zuur et al. 2003, 2007). Dynamic factor analysis is based on structural time-series models (Jalles 2009). The trend for a structural time series model, such as

Time series = constant + trend + explanatory variables + noise

is modeled as a smoothing curve, based on a Kalman filter/smoothing algorithm. The 'explanatory variable' component is modeled as linear regression (Zuur and Pierce 2004; Zuur et al. 2003). Dynamic factor analysis estimates a linear combination of M common trends of all N time series and can be written in matrix notation as:

$$y_t = Az_t + Bx_t + e_t$$

where the N x M matrix A contains the factor loadings, z_t the trend, B the regression parameters, x_t the value of the explanatory variable, and e_t the noise components (Zuur et al. 2003; Zuur and Pierce 2004). Magnitude and sign of factor loadings determine how the common trends are related to the original time series.

Prior the DFA, monthly means of SST and air temperature data were de-seasonalized using the standard procedure "Seasonal decomposition by LOESS" in Brodgar (v.2.6.6), to eliminate the strong seasonal signals within these data sets. SAM and ENSO indices were taken as explanatory variables. Data were checked for normality using QQ-Plots for the original time series, for square root, cubic root and $\log_{10}$ transformed data. All plots indicated that the original data are almost normally distributed and that transformations do not considerably improve normality of the data set. While normality of data is generally beneficial in DFA models, it is not a prerequisite (Zuur et al. 2003). Table 1 shows the four dynamic factor models that were used in our analysis. As explanatory variables, both climate indices SAM and ENSO and their combination were applied. The maximum of three common trends was calculated. Regarding the modeling of the error covariance matrix R, the simplest approach is to use a diagonal matrix. Alternatively, a symmetric, non-diagonal

Table 1 The four dynamic factor models used in the analysis. R is the error covariance matrix

No.	Model	R
1	data = M common trends + noise	diagonal
2	data = M common trends + explanatory variable + noise	diagonal
3	data = M common trends + noise	non-diagonal
4	data = M common trends + explanatory variable + noise	non-diagonal

matrix for R can be used (Zuur et al. 2003) Off-diagonal elements of R represent the information in the response variables which cannot be explained with the other terms (Zuur et al. 2003; Zuur and Pierce 2004). We applied different models which i) yield one, two or three "model-specific" common trends (see column M in Table 3); ii) models with and without explanatory variables (SAM, ENSO). An overview of all tested models is given in Table 3. To decide which model fits the data best, Akaike's information criterion (AIC) was used and calculated for each possible combination of explanatory variables. The model with the smallest AIC is chosen as the optimal fit (Akaike 1974).

3 Results

3.1 U-statistics and turning points

Maximum values of the U statistics are summarized in Table 2. Taking into account the critical values listed in Buishand (1984), it is possible to detect abrupt changes. In the present data set, the Buishand U indicates abrupt changes (= turning points) in SST with a significance level $\alpha=0.01$ and salinity with a significance level $\alpha=0.05$. In TSPM and Chl a the null hypothesis (no abrupt change over time) cannot be rejected, although in TSPM the U values is close to 90 % significance (cf. Buishand 1984).

For the calculation of U_t only the available values of each parameter were included and missing values were ignored, leading to a condensed data set, where the numbering of the month is not consistent with the calendar month. To enhance understanding, the actual calendar month is given in parenthesis throughout the text.

SST shows a clear change-point at month 82 (i.e. May 2009) where U_t has its maximum (Fig. 3a). Before this time point, the mean SST is −0.093 °C±0.04 °C SE (November 1991–April 2009) and changes to −0.423 °C±0.03 °C SE thereafter (June 2009–December 2010). The analysis suggests a slight decrease in SST after May 2009. Sea surface salinity also shows a turning point (Fig. 3b), in this case at month 15 (i.e. December 1993). After this point in the series the mean salinity shifts from 34.04 psu±0.07 psu SE to 33.77 psu±0.05 psu SE.

While the statistic U indicated no turning point in the Chl a data set, the U_t revealed two potential shifts in the mean, i.e. rather a tiered decrease. The first shift appears after month 20 (i.e. December

Table 2 Summary of statistical indices U calculated for four parameters. n gives the number of measured values. Significance on the 95 % level is marked with *, on the 99 % level with **

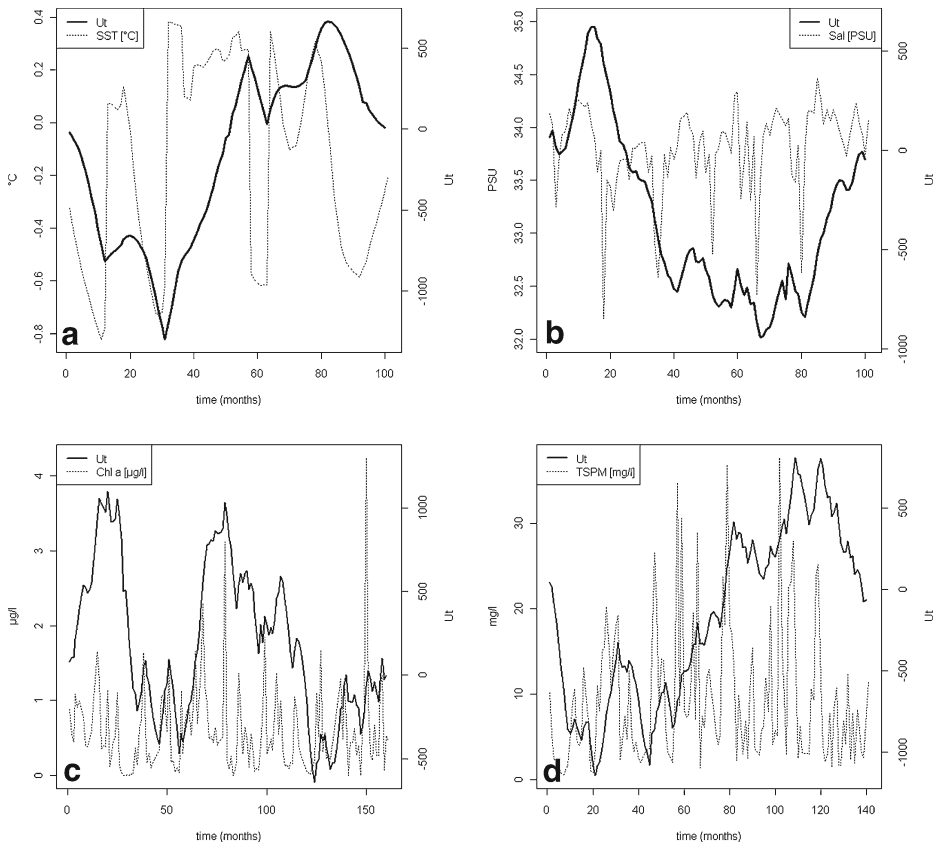|	n	U
SST	101	0.923**
Salinity	101	0.551*
Chl a	161	0.095
TSPM	141	0.318

Fig. 3 Plot of monthly means of parameters and according calculated U_t values against time (month). **a** de-seasonalized SST, **b** Salinity, **c** Chl a, **d** TSPM. Only available monthly means were taken into account, missing values were left out

1993), the second one after month 79 (i.e. April 2002, see Fig. 3c). The mean Chl a content decreases from 0.772 μg/l±0.09 μg/l SE before December 1993 to 0.581 μg/l±0.07 μg/l SE between December 1993 and April 2002, and to 0.549 μg/l±0.07 μg/l SE after April 2002 until December 2010.

In TSPM two maximum peaks close to each other (see Fig. 3d) make it impossible for the *U-statistics* to detect a clear change in the mean. However, the absolute maximum U_t value was calculated for month 109 (= April 2008). The second highest U_t value was calculated for month 120 (= March 2009). Before April 2008, the mean of TSPM can be quantified with 9.87 mg/l±0.80 mg/l SE, whereas after March 2009 it decreases to 5.48 mg/l±0.76 mg/l SE for the rest of the data set until December 2010.

3.2 Additive modeling

We observed a highly significant non-linear relationship between SST and year ($F=16.87$, $p<0.001$), with all the explanatory variables air temperature, ENSO and SAM having a significant influence: air temperature ($p=0.022$), SAM (p 0.005) and ENSO ($p<0.001$). The model SST ~ 1 + air temperature + SAM + ENSO + s(year) explains 72.6 % of the total
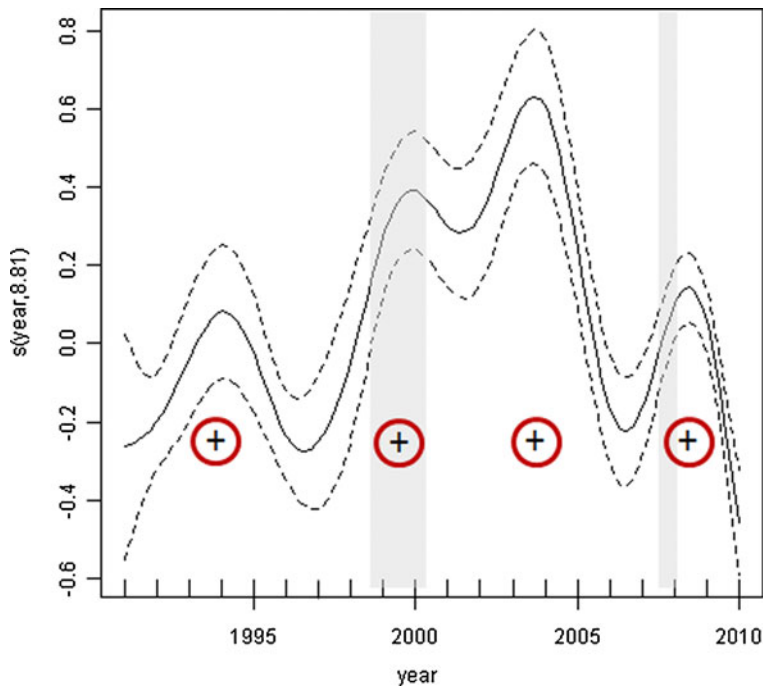
Fig. 4 Smoothing curve *s(year)* for SST data with 8.81° of freedom and air temperature, SAM and ENSO as explanatory variables. The *solid line* is the smoother; the *dotted lines* 95 % confidence bands. *Shaded bars* indicate strong La Niña events, + indicates + SAM events

variation in the SST data set. Visualization of the model (Fig. 4) clearly reveals an ENSO and SAM-related cyclic pattern. Positive peaks in SST can generally be attributed to + SAM events and/or strong La Niña events, which cause warmer conditions with less sea ice in the WAP region (Stammerjohn et al. 2008; Martinson et al. 2008; Brey et al. 2011). The threshold for a strong La Niña was at −1, for a strong SAM + at least two subsequent months with an index >100. Salinity is significantly influenced by ENSO ($p=0.026$), again with a significant non-linear relationship between salinity and year as a smoohthing function ($F=3.193, p=0.020$). The resulting model Salinity ~ 1+ ENSO + s(year) explains only 18.2 % of the variation, and the confidence intervals of the model are too wide to interpret it sufficiently. Therefore, we chose to reject the model. In the Chl *a* content and TSPM data series no influence of either air temperature, SAM or ENSO can be detected (Figure 5).

3.3 Dynamic factor analysis (DFA)

The model that best fits our dataset is the model with the two common trends depicted in Fig. 4 and using both SAM and ENSO as explanatory variables with a diagonal error covariance matrix **R** (model 2 h with AIC = 1408.24, see Table 3).

The two best defined common trends (model 2 h) are presented in Fig. 4a and b. In the first common trend a strongly negative peak is visible at month 10 (i.e. August 1992), followed by a long phase with four positive peaks around months 45 (July 1995), 88 (February 1999), 190 (August 2007) and 210 (April 2009). A positive phase in the middle (month 120–164, i.e. October 2001–July 2005) is turning into a final negative trend phase
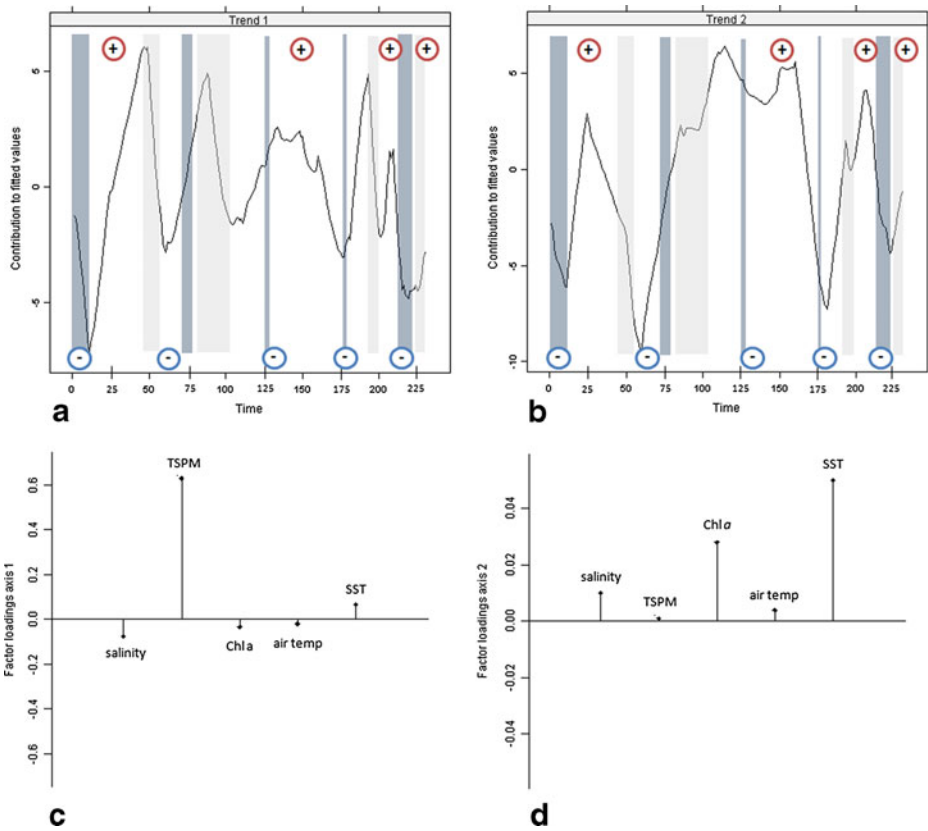
Fig. 5 Common trends and factor loadings as results of a dynamic factor analysis, based on the 19-year data set with the variables SST, salinity, Chl *a*, TSPM and air temperature, and SAM and ENSO as explanatory variables: **a**, **b** common trends of the long-term data set, *shaded bars* represent El Niño (*dark grey*) and La Nina (*light grey*) events. + and − represent + SAM and –SAM phases. **c**, **d** factor loadings representing the main driver of the according common trend

(month 214–228, i.e. August 2009–October 2010). In the second trend (Fig. 4b), cyclic patterns become visible with negative peaks after months 10 and 60 (i.e. August 1992 and December 1995), a long positive phase between months 70 and 160 (i.e. January 1996 and mid-October 2005), and strong negative peaks again around month 180 (December 2005) and month 220 (i.e. February 2010). The pronounced negative peaks at the beginning (August 1992) and the end (February 2010) are visible in both trends. The magnitude of the factor loadings determines how the common trends are related to the original data series (Zuur and Pierce 2004). Here, the factor loadings for both trends (Fig. 4c, d) demonstrate that TSPM is mainly driven by the first trend, while SST, Chl *a* and salinity are mainly driven by the second trend. Generally, we can state that the TSPM trend is high during + SAM events, which are often in phase with La Niña events. Strong negative peaks in TSPM are related to -SAM/El Niño events. The forces that are driving the second trend, i.e. mainly SST, Chl *a* and salinity, are not quite as clear as for TSPM. But generally speaking this trend is also positive during + SAM/La Niña, whereas it is negative during strong -SAM/El Niño.

Table 3 AIC values obtained by applying dynamic factor analysis models 1 to 4 on the time series. M indicates the number of common trends of the model

Model	M	Explanatory variable	AIC
1a	1	–	1498.36
1b	2	–	1485.83
1c	3	–	1494.57
2a	1	SAM	1411.25
2b	2	SAM	1689.25
2c	3	SAM	1425.83
2d	1	ENSO	1498.15
2e	2	ENSO	1484.07
2f	3	ENSO	1496.00
2g	1	SAM + ENSO	1418.24
2h	2	SAM + ENSO	1408.24
2i	3	SAM + ENSO	1413.28
3a	1	–	1503.42
3b	2	–	1497.45
3c	3	–	1500.84
4a	1	SAM	1416.83
4b	2	SAM	1640.43
4c	3	SAM	1433.73
4d	1	ENSO	1506.15
4e	2	ENSO	1508.14
4f	3	ENSO	1505.21
4g	1	SAM + ENSO	1425.01
4h	2	SAM + ENSO	1417.10
4i	3	SAM + ENSO	1442.25

4 Discussion

This analysis of our 20-year hydrographical data set, using specific tests of turning points and analyses of non-linear trends, was aimed to gain more detailed insight into the climatic drivers of hydrographic change observed in the coastal systems at King George Island (WAP). Despite the fact that trend analyses, or analyses of change of time series of less than 30 years, are often considered too limited to allow reliable modeling (Kundzewicz and Robson 2004), our methods not only reveal sudden changes for most parameters, but also cyclic patterns that can be related to climatic oscillations such as SAM and ENSO.

Using the *U-statistics* after Buishand (1984), we detected sudden changes, i.e. significant shifts in the mean values within the existing 19y-time series, as a proxy for climate cycles. By additionally applying the *U-statistics* after Pettitt (1980, 1981), we were able to date these sudden changes of SST to after May 2009 and of salinity and Chl *a* to after December 1993. Before May 2009, SST in Potter Cove was increasing, as demonstrated by Schloss et al. (2012) for the summer values. A strong El Niño event in 2009/2010 caused substantial cooling which led to a decrease in SST. A continuous trend of increasing SST over the past decades before 2009 in the WAP region has been detected in several studies (e.g. Meredith and King 2005; Stammerjohn et al. 2008, amongst others). As SST is rising, salinity in

coastal areas tends to decrease due to surface dilution with enhanced quantities of glacial melt water. Under experimental conditions simulating glacial influence (higher water temperature and decreased salinity) stress effects on phytoplankton production and, hence, Chl *a* accumulation (a proxy for phytoplankton biomass) as well as on algal fitness parameters has been documented to last at least several weeks (M. Hernando, *unpubl. data.*). Our findings of a sudden change in mean SST, with a lower mean after May 2009 coincide with a strong El Niño starting only 1 month later. The strong influence of ENSO on the WAP region is well defined (Murphy et al. 2007; Yuan 2004). A warm ENSO phase (El Niño) in the Pacific leads to cooling in the WAP region, entailing an increase of sea ice extent and duration (Stammerjohn et al. 2008; Brey et al. 2011). The decrease of TSPM after March 2009 can also be related to the influence of this strong El Niño event, since in March (austral autumn) glacial melting usually ceases and the El Niño started directly at the beginning of winter. This coincidence resulted in El Niño influence persisting into the austral summer 2009/2010, during which glacier melt was less intense than in previous years and, hence, resulted in less TSPM production from melt water inflow. This would also underline that glacier melting and not bottom re-suspension is the major driver of TSPM concentrations in surface waters of Potter Cove. The reason why similar effects could not be shown during previous strong El Niño events, e.g. 1991/92 and 1997/98, may be attributed to the increasing quality of the data set, with a more constant sampling scheme after 2000, as well as the fact that all El Niño events are different (Meredith et al. 2008).

Extrapolating the short-term effect to the natural conditions, this freshening may abate plankton biomass in the water column corroborated by slightly decreasing salinity and Chl *a* content from 1993 onwards. Montes-Hugo et al. (2009) and Schloss et al. (2012) both report a decrease in summer Chl *a* values at the WAP. Both GAM and DFA revealed the clear impact of climate oscillations, SAM and/or ENSO on SST, Chl *a* and TSPM. Whereas in our previous analysis (Schloss et al. 2012) the influence of either SAM or ENSO was mainly detected in the outer Potter Cove, now with the GAM and DFA analyses we are able to show the influence of climatic forcing even in the inner cove, close to the glacier. In contrast to our previous work (Schloss et al. 2012) which implied a rather slight but steady increase in SST, the GAM actually resolves the underlying climatic patterns. The DFA reveals main components affected by the climatic cycles, namely SST and TSPM. The latter is directly linked to the melt water run-off from the glaciers.

Both SAM and ENSO have shown long-period changes in frequency, intensity and duration (Meredith et al. 2008), leading to a dominance of positive SAM and/or La Niña conditions from the late 1980 onwards (Stammerjohn et al. 2012). Therefore, changes in the coastal ecosystems of the WAP region are to be expected, particularly since the climate cycles appear to have a great influence on SST and other parameters. The ensuing decrease in phytoplankton biomass, as documented by the changes in Chl *a* content and/or species composition (Schofield et al. 2010), is bound to have important effects on the zooplankton community composition and abundance and hence on the pelagic food web.

The second common trend identified by the DFA, manifesting mainly in changes of SST and Chl *a* content, peaks low immediately before and during the very strong El Niño events 1991/92, 1997/98, and 2009, interrupted by a phase of high values in the 2000–2002 years. Similar patterns were observed in the Chl *a* concentrations around Elephant Island, South Shetland Islands (Loeb et al. 2010). According to Loeb et al. (2010), there was a decade-long regime shift after the 1997/98 El Niño towards a phase with more frequent La Niña and weak El Niño events, causing a shift in the zooplankton community with high abundances of copepods and salps displacing the krill. This species shift is also observed at Carlini Station where the last massive krill biomasses were observed around 2005 and afterwards replaced by salps (personal observations, Abele). Martinson et al. (2008) attribute this regime shift to the substantially increased advection of warm Upper Circumpolar Deep Water (UCDW) onto the shelf after the

1998 El Niño event. This shift is further promoted by an extraordinary storm event in 2002, which lead to an intrusion of anomalously warm water onto the WAP shelf (Martinson et al. 2008; Turner et al. 2002). This intrusion of warm water may have minimized the cooling effect of –SAM/El Niño, visible in our DFA (Fig. 4a, b: month 125–136, i.e. March 2002–Feb 2003).

Our results emphasize the strong influence of climatic oscillations in the northern WAP region. Although our study site is located in a shallow coastal environment, the signs of climatic oscillations can be detected. Whereas in a seminal analysis of the first part of the present data set (Schloss et al. 2012) the effects of SAM and ENSO appeared to be conditioned by the distinct local characteristics of the inner Potter Cove environment such as rather shallow bathymetry, and a higher input of both freshwater and suspended particles due to glacier melting, the present statistical analyses clearly confirms the strong influence of SAM and ENSO upon local trends. Importantly, in the analysis of Schloss et al. (2012) the environmental variables were individually correlated with different climatic drivers, such as air temperature, SAM and ENSO. These environmental variables are, however, interdependent and physically connected, and the present analysis statistically combines all measured variables with the climatic drivers. By combining the variables, the analyses (GAM, DFA) not only revealed the dominating cyclic patterns, but also highlight how the variables are related. While our previous analyses assumed a rather linear relation between the single variables and climatic drivers (Schloss et al. 2012), our present analysis unveils the climatically dynamics *in* the variables and is therefore more powerful in describing the response of the Potter Cove pelagic system. The "tipping points" and sudden changes in the time series, as detected by the *U-statistics*, are important because they give insights in how and when changes in the system occur. As our study forms part of an ecological long-term program, the analysis may help to interpret time dependent shifts in pelagic and benthic ecosystem compartments investigated by other groups in Potter Cove.

Long-term data series are required for the interpretation of hydrographic and other environmental data in the light of large climatic phenomena (like the SAM and ENSO, or other oscillations). Since such series are often incomplete and also mostly just at the beginning and short at many Antarctic platforms (stations, permanent monitoring installations), our statistical analyses may prove applicable for many similar data sets from other areas. The analysis also shows, how important it is to continue the monitoring of hydrographical parameters to further examine climate trends and cycles in the face of global climate change, and to link the Carlini data sets with other monitoring stations along the Western Antarctic Peninsula such as the Long Term Ecological Research at Palmer Station (Pal LTER) and the Rothera measuring station (RaTS, British Antarctic Survey). This will increase the observational density and spatial resolution of climate change trends along WAP, for a better understanding of the regional variability of climate change and its impacts on coastal and shelf systems.

References

Akaike H (1974) A new look at the statistical identification model. IEEE Trans Autom Control 19:716–723

Blindow N, Suckro SK, Rückamp M, Braun M, Schindler M, Breuer B, Saurer H, Simoes JC, Lange MA (2010) Geometry and thermal regime of the King George Island ice cap, Antarctica, from GPR and GPS. Ann Glaciol 51(55):103–109

Brey T, Voigt M, Jenkins K, Ahn I-Y (2011) The bivalve Laternula elliptica at King George Island—a biological recorder of climate forcing in the West Antarctic Peninsula region. J Mar Syst 88(4):542–552. doi:10.1016/j.jmarsys.2011.07.004

Buishand TA (1984) Tests for detectung a shift in the mean of hydrological time-series. J Hydrol 73(1–2):51–69

Caloiero T, Coscarelli R, Ferrari E, Mancini M (2011) Trend detection of annual and seasonal rainfall in Calabria (Southern Italy). Int J Climatol 31(1):44–56. doi:10.1002/joc.2055

Clarke A, Griffiths HJ, Barnes DKA, Meredith MP, Grant SM (2009) Spatial variation in seabed temperatures in the Southern Ocean: implications for benthic ecology and biogeography. J Geophys Res Biogeosci 114. doi:10.1029/2008jg000886

Cleveland RB, Cleveland WS, McRae JE, Terpenning I (1990) A seasonal-trend decomposition procedure based on loess. J Off Stat 6:3–73

Ducklow HW, Baker K, Martinson DG, Quetin LB, Ross RM, Smith RC, Stammerjohn SE, Vernet M, Fraser W (2007) Marine pelagic ecosystems: the West Antarctic Peninsula. Philos Trans R Soc B Biol Sci 362 (1477):67–94

Eraso A, Dominguez MdC (2007) Physicochemical characteristics of the subglacier discharge in Potter Cove, King George Island, Antarctica. vol 45. University of Silesia, Wroclaw

Fogt RL, Bromwich DH, Hines KM (2011) Understanding the SAM influence on the South Pacific ENSO teleconnection. Clim Dyn 36(7–8):1555–1576. doi:10.1007/s00382-010-0905-0

Gillet NP, Kell TD, Jones PD (2006) Regional climate impacts of the southern annular mode. Geophys Res Lett 33:L23704. doi:10.1029/2006GL027721

Gong DY, Wang SW (1999) Definition of antarctic oscillation index. Geophys Res Lett 26(4):459–462. doi:10.1029/1999gl900003

Hastie T, Tibshirani R (1986) Generalized additive models (with discussion). Stat Sci 1:297–318

Jalles JT (2009) Structural time series models and the Kalman Filter: a concise review. FEUNL Work Pap 541. doi:10.2139/ssrn.1496864

Kiely G, Albertson JD, Parlange MB (1998) Recent trends in diurnal variation of precipitation at Valentia on the west coast of Ireland. J Hydrol 207(3–4):270–279

Kundzewicz Z, Robson AJ (2004) Change detection in hydrological records—a review of the methodology. Bull Hydrol 49(1):7–19

Loeb V, Hofmann EE, Klinck JM, Holm-Hansen O (2010) Hydrographic control of the marine ecosystem in the South Shetland-Elephant Island and Bransfield Strait region. Deep-Sea Res II Top Stud Oceanogr 57 (7–8):519–542. doi:10.1016/j.dsr2.2009.10.004

Marshall GJ (2002) Analysis of recent circulation and thermal advection change in the northern Antarctic Peninsula. Int J Climatol 22(12):1557–1567. doi:10.1002/joc.814

Marshall GJ (2007) Half-century seasonal relationships between the Southern Annular Mode and Antarctic temperatures. Int J Climatol 27(3):373–383. doi:10.1002/joc.1407

Martinson DG, Stammerjohn SE, Iannuzzi RA, Smith RC, Vernet M (2008) Western Antarctic Peninsula physical oceanography and spatio-temporal variability. Deep-Sea Res II Top Stud Oceanogr 55(18–19):1964–1987. doi:10.1016/j.dsr2.2008.04.038

Meredith MP, King JC (2005) Rapid climate change in the ocean west of the Antarctic Peninsula during the second half of the 20th century. Geophys Res Lett 32(19). doi:10.1029/2005gl024042

Meredith MP, Murphy EJ, Hawker EJ, King JC, Wallace MI (2008) On the interannual variability of ocean temperatures around South Georgia, Southern Ocean: forcing by El Nino/Southern Oscillation and the Southern Annular Mode. Deep-Sea Res II Top Stud Oceanogr 55(18–19):2007–2022. doi:10.1016/j.dsr2.2008.05.020

Monaghan AJ, Bromwich DH, Chapman W, Comiso JC (2008) Recent variability and trends of Antarctic near-surface temperature. J Geophys Res Atmos 113(D4). doi:10.1029/2007jd009094

Montes-Hugo M, Doney SC, Ducklow HW, Fraser W, Martinson D, Stammerjohn SE, Schofield O (2009) Recent Changes in Phytoplankton Communities Associated with Rapid Regional Climate Change Along the Western Antarctic Peninsula. Science 323 (5920):1470–1473. doi:10.1126/science.1164533

Monien P, Schnetger B, Brumsack HJ, Hass HC, Kuhn G (2011) A geochemical record of late Holocene palaeoenvironmental changes at King George Island (maritime Antarctica). Antarct Sci 23(3):255–267. doi:10.1017/s095410201100006x

Murphy EJ, Watkins JL, Trathan PN, Reid K, Meredith MP, Thorpe SE, Johnston NM, Clarke A, Tarling GA, Collins MA, Forcada J, Shreeve RS, Atkinson A, Korb R, Whitehouse MJ, Ward P, Rodhouse PG, Enderlein P, Hirst AG, Martin AR, Hill SL, Staniland IJ, Pond DW, Briggs DR, Cunningham NJ, Fleming AH (2007) Spatial and temporal operation of the Scotia Sea ecosystem: a review of large-scale links in a krill centred food web. Philos Trans R Soc B Biol Sci 362(1477):113–148. doi:10.1098/rstb.2006.1957

Orr A, Marshall GJ, Hunt JCR, Sommeria J, Wang CG, van Lipzig NPM, Cresswell D, King JC (2008) Characteristics of summer airflow over the Antarctic Peninsula in response to recent strengthening of westerly circumpolar winds. J Atmos Sci 65(4):1396–1413. doi:10.1175/2007jas2498.1

Pakhomov EA, Fuentes V, Schloss I, Atencio A, Esnal GB (2003) Beaching of the tunicate Salpa thompsoni at high levels of suspended particulate matter in the Southern Ocean. Polar Biol 26(7):427–431. doi:10.1007/s00300-003-0494-z

Pettitt AN (1980) Some results on estimating a change-point using nonparametric type statistics. J Stat Comput Simul 11(3–4):261–272

Pettitt AN (1981) Posterior probabilities for a change-point using ranks. Biometrika 68(2):443–450

Philipp EER (2010) Suspended paticulate matter measured at three station in Potter Cove, King George Island, Western Antarctic Peninsula. doi:10.1594/PANGAEA.746016

Rückamp M, Braun M, Suckro S, Blindow N (2011) Observed glacial changes on the King George Island ice cap, Antarctica, in the last decade. Global and Planetary Change in press (available online 6 July 2011). doi:10.1016/j.gloplacha.2011.06.009

Russell A, McGregor GR (2010) Southern hemisphere atmospheric circulation: impacts on Antarctic climate and reconstructions from Antarctic ice core data. Clim Chang 99(1–2):155–192. doi:10.1007/s10584-009-9673-4

Schloss IR, Ferreyra GA, Mercuri G, Kowalke J (1999) Particle flux in an Antarctic shallow coastal environment: a sediment trap study. Sci Mar 63:99–111

Schloss IR, Abele D, Moreau S, Demers S, Bers AV, Gonzáles O, Ferreyra GA (2012) Response of phytoplankton dynamics to 19-year (1991–2009) climate trends in Potter Cove (Antarctica). J Mar Syst 92:53–66. doi:10.1016/j.jmarsys.2011.10.006

Schofield O, Ducklow HW, Martinson DG, Meredith MP, Moline MA, Fraser WR (2010) How do polar marine ecosystems respond to rapid climate change? Science 328(5985):1520–1523. doi:10.1126/science.1185779

Smith CA, Sardeshmukh P (2000) The effect of ENSO on the intraseasonal variance of surface temperature in winter. Int J Climatol 20:1543–1557

Smith RC, Martinson DG, Stammerjohn SE, Iannuzzi RA, Ireson K (2008) Bellingshausen and western Antarctic Peninsula region: pigment biomass and sea-ice spatial/temporal distributions and interannual variabilty. Deep-Sea Res II Top Stud Oceanogr 55(18–19):1949–1963. doi:10.1016/j.dsr2.2008.04.027

Stammerjohn SE, Martinson DG, Smith RC, Yuan X, Rind D (2008) Trends in Antarctic annual sea ice retreat and advance and their relation to El Nino-Southern Oscillation and Southern Annular Mode variability. J Geophys Res Oceans 113(C3). doi:10.1029/2007jc004269

Stammerjohn S, Massom R, Rind D, Martinson D (2012) Regions of rapid sea ice change: an inter-hemispheric seasonal comparison. Geophys Res Lett 39. doi:10.1029/2012gl050874

Tatian M, Sahade R, Mercuri G, Fuentes VL, Antacli JC, Stellfeldt A, Esnal GB (2008) Feeding ecology of benthic filter-feeders at Potter Cove, an Antarctic coastal ecosystem. Polar Biol 31(4):509–517. doi:10.1007/s00300-007-0379-7

Turner J, Harangozo SA, Marshall GJ, King JC, Colwell SR (2002) Anomalous atmospheric circulation over the Weddell Sea, Antarctica during the Austral summer of 2001/02 resulting in extreme sea ice conditions. Geophys Res Lett 29(24). doi:10.1029/2002gl015565

Turner J, Colwell SR, Marshall GJ, Lachlan-Cope TA, Carleton AM, Jones PD, Lagun V, Reid PA, Iagovkina S (2005) Antarctic climate change during the last 50 years. Int J Climatol 25(3):279–294

Vaughan DG (2006) Recent trends in melting conditions on the Antarctic Peninsula and their implications for ice-sheet mass balance and sea level. Arct Antarct Alp Res 38(1):147–152

Vaughan DG, Marshall GJ, Connolley WM, Parkinson C, Mulvaney R, Hodgson DA, King JC, Pudsey CJ, Turner J (2003) Recent rapid regional climate warming on the Antarctic Peninsula. Clim Chang 60(3):243–274

Wood SN (2006) Generalized additive models–an introduction with R. Chapmann & Hall/CRC, Boca Raton

Yuan XJ (2004) ENSO-related impacts on Antarctic sea ice: a synthesis of phenomenon and mechanisms. Antarct Sci 16(4):415–425. doi:10.1017/s0954102004002238

Zuur AF, Pierce GJ (2004) Common trends in northeast Atlantic squid time series. J Sea Res 52(1):57–72. doi:10.1016/j.sears.2003.08.008

Zuur AF, Fryer RJ, Jolliffe IT, Dekker R, Beukema JJ (2003) Estimating common trends in multivariate time series using dynamic factor analysis. Environmetrics 14(7):665–685. doi:10.1002/env.611

Zuur AF, Ieno EN, Smith GM (2007) Analysing ecological data. Statistics for biology and health. Springer, New York

Zuur AF, Ieno EN, Walker NJ, Saveliev AA, Smith GM (2009) Mixed effects models and extensions in ecology with R. Statistics for biology and health. Springer, New York